Original Article

Journal of Intelligent Material Systems and Structures

Journal of Intelligent Material Systems and Structures
2014, Vol. 25(14) 1681–1692

DOI: 10.1177/1045389X14541501
jim.sagepub.com
SAGE

Piezoelectret foam–based vibration energy harvesting

SR Anton[1], KM Farinholt[2] and A Erturk[3]

Abstract

The use of energy harvesting to provide power to low-power electronic devices has the potential to create autonomous, self-powered electronics. This article presents the investigation of a novel material for vibration-based energy harvesting. Piezoelectret foam, a lead-free, polymer-based electret material exhibiting piezoelectric-like properties, is investigated for low-power energy generation. An overview of the fabrication and operation of piezoelectret foams is first given. Mechanical testing is then performed, where anisotropy in the principal length directions is found along with Young's moduli between 0.5 and 1 GPa and tensile strengths from 35 to 70 MPa. Dynamic electromechanical characterization is performed in order to measure the piezoelectric d_{33} coefficient of the foam over a wide frequency range. The d_{33} coefficient is found to be relatively constant at around 175 pC/N from 10 Hz to 1 kHz. Finally, the foam is evaluated as an energy harvesting material by first developing an electromechanical model to predict the voltage response during excitation, then performing dynamic experimentation to measure the voltage frequency response with comparisons to modeling predictions for a set of electrical loads, and finally conducting energy harvesting experimentation in which the foam is used to charge a capacitor. Harmonic excitation of a pre-tensioned 15.2 cm $\times$ 15.2 cm sample at 60 Hz and displacement of $\pm$ 73 μm yields an average power of 6.0 μW delivered to a 1 mF storage capacitor. The capacitor is charged to 4.67 V in 30 min, proving the ability of piezoelectret foam to supply power to small electronic components.

Keywords

Energy harvesting, piezoelectret foam, electromechanical model, piezoelectric

Introduction

Harvesting ambient energy to supply power to low-power electronics, such as wireless sensors, has gained tremendous interest in the research community in the last decade. With advancements leading to the reduction of power demands of electronic devices combined with developments in the field of energy harvesting, it is becoming feasible to create self-powered autonomous devices. Researchers have investigated scavenging several sources of ambient energy, including wind, solar, thermal, and vibration energy, using a multitude of transduction mechanisms and materials. Vibration energy harvesting, particularly using piezoelectric materials, constitutes a majority of the work in low-level energy harvesting (Anton and Sodano, 2007; Beeby et al., 2006; Cook-Chennault et al., 2008; Sodano et al., 2004).

The most common piezoelectric material investigated is the ceramic lead zirconate titanate (PZT), thanks to its large piezoelectric coupling coefficient resulting in relatively large energy output compared to other piezoelectric materials. While PZT is a popular material, its brittle nature presents limitations in use. Alternatively, more compliant piezoelectric materials such as piezoceramic fiber–based composites and polymer-based piezoelectrics can be considered. The most common polymer piezoelectric material investigated is polyvinylidene fluoride (PVDF), which possess a relatively low coupling coefficient and flexible nature.

In this work, a novel piezoelectric polymer material, namely cellular polypropylene piezoelectret foam, is considered for vibration energy harvesting applications. Piezoelectret foams have been used in sensing applications for some time, but present a novel material for energy harvesting purposes. A detailed comparison of

[1]Department of Mechanical Engineering, Tennessee Technological University, Cookeville, TN, USA
[2]Luna Innovations, Inc., Charlottesville, VA, USA
[3]George W. Woodruff School of Mechanical Engineering, Georgia Institute of Technology, Atlanta, GA, USA

Corresponding author:
SR Anton, Department of Mechanical Engineering, Tennessee Technological University, Cookeville, TN 38505, USA.
Email: santon@tntech.edu

Table 1. Comparison of several piezoelectric materials and their properties.

	Piezoelectret foam	PVDF	PZT	PMN-PZT
Density (kg/m^3)	1000	1780	7500	7000
Piezoelectric constant (pC/N)	25–250 (d_{33})	−33 (d_{33})	600 (d_{33})	2000 (d_{33})
Advantages	Very lightweight, very flexible	Lightweight, flexible	High coupling	Very high coupling
Disadvantages	Medium coupling	Low coupling	Heavy, brittle	Heavy, very brittle

PVDF: polyvinylidene fluoride; PZT: lead zirconate titanate; PMN-PZT: lead magnesium niobate–lead zirconate titanate.

various piezoelectric polymers including piezoelectret foam and PVDF is given by Ramadan et al. (2014). For convenience, a summary comparison of piezoelectret foam with PVDF, conventional PZT, and single-crystal lead magnesium niobate–lead zirconate titanate (PMN-PZT) is given here in Table 1. An advantage of piezoelectret foam over PZT-based ceramics is its lead-free, environmentally benign composition while offering comparable piezoelectric constant levels with much lower mass density. Perhaps one of the most significant drawbacks of piezoelectret foam is its limited thermal stability. The piezoelectric properties of cellular polypropylene piezoelectrets have been shown to degrade above 50°C; therefore, they are restricted to use in moderate temperature environments (Neugschwandtner et al., 2001). The long-term stability of piezoelectret foams at room temperature is also of concern, although studies have shown stable piezoelectric properties after 200 days (Mellinger et al., 2006). Potential application fields for piezoelectret foam energy harvesting may include harvesting vibration energy in mass-sensitive systems such as unmanned aerial vehicles, harvesting energy from curved surfaces such as pipelines, wind turbine blades, and/or towers, and harvesting energy for biomedical applications, which require extremely compliant harvesters.

Piezoelectret foams are a class of electret material, a dielectric material that contains permanent electric charge, or polarization analogous to the magnetic fields found in permanent magnets. Piezoelectricity is observed in piezoelectrets due to the deposition of charge on internal voids in the structure. A scanning electron microscope (SEM) image showing the microstructure of a typical piezoelectret foam is given in Figure 1, in which lens-like voids can be observed. When subject to mechanical or electrical stimuli, the charged voids respond as macroscopic dipoles, thus yielding piezoelectric-like properties.

Piezoelectret foams were first developed in the 1980s at Tampere University of Technology in Finland and later at the Technical Research Centre of Finland (VTT) (Savolainen and Kirjavainen, 1989). Although several polymer materials can be used to create piezoelectrets, polypropylene is the most common material used (Wegener and Bauer, 2005). Since the 1990s, a large amount of research has been presented on the investigation of cellular polypropylene piezoelectric material. Studies have investigated electrostatic modeling of the material (Hillenbrand and Sessler, 2000; Paajanen et al., 1999, 2000b; Sessler and Hillenbrand, 1999), experimental measurement of the piezoelectric properties of piezoelectrets and validation of the various models (Hillenbrand et al., 2005; Hillenbrand and Sessler, 2004; Kressmann, 2001; Neugschwandtner et al., 2000, 2001; Paajanen et al., 2000a), and methods for improving the piezoelectric constant, d_{33}, via expansion processes and altering the gas used in the air gaps during charging (Paajanen et al., 2001, 2002; Zhang et al., 2004a, 2004b). Several review articles on ferroelectrets have also been published (Bauer et al., 2004; Gerhard-Multhaupt, 2002; Wegener and Bauer, 2005). Additionally, several studies have looked at using piezoelectrets in electrostatic energy harvesting systems. These studies, many of which are summarized by Boisseau et al. (2010), consider a piezoelectret to act as one face of an electrostatic energy harvester. The permanent charge on the piezoelectret material allows the harvester to operate without pre-charge. While this electrostatic technique still harvests vibration energy use of piezoelectrets in electrostatic harvesters does not take advantage of the inherent piezoelectricity of the material. Few studies have investigated the direct use of the relatively large d_{33} coefficient of piezoelectrets to harvest mechanical energy.

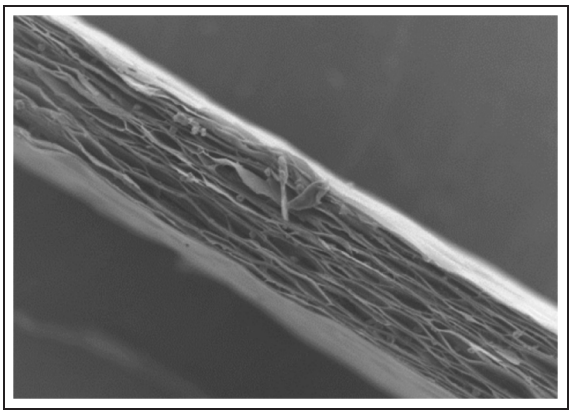

Figure 1. Scanning electron microscope image of piezoelectret foam microstructure showing lens-like voids. Thickness of sample is approximately 70 μm.
Source: Reproduced with permission by Emfit Inc.

Several aspects of piezoelectret foams and their use in vibration energy harvesting are discussed in this work in the following manner. First, the basic fabrication and transduction mechanism of piezoelectrets are discussed. Results of mechanical tensile testing of several piezoelectret foam samples are then given. Next, dynamic testing of the piezoelectric d_{33} coefficient is described and results are compared to those found in the literature. The use of piezoelectret foam for low-level vibration energy harvesting is then explored. An electromechanical model is developed to predict the electrical behavior of the foam in response to mechanical excitation in the presence of a resistive electrical load. Experimental frequency response functions (FRFs) are measured and compared to the model predictions. Additionally, experimentation in which harmonic excitation of a pre-tensioned foam sample along the length direction is performed and a simple full-wave rectifier electronic circuit is used to charge a capacitor. Finally, conclusions are made regarding the use of piezoelectret foam in vibration energy harvesting systems.

Overview of piezoelectret foam

Formation of piezoelectret foam involves a process in which biaxial stretching of polypropylene (other polymers can be used as well) forms lens-like voids in the material (Gerhard-Multhaupt, 2002). Before stretching, the material may be foamed using a chemical process or can contain mineral particles, which act as initiation sites for the voids during stretching. A cross-sectional schematic of piezoelectret foam is shown in Figure 2(a), in which the voids are clearly illustrated. Once stretched, the foam is charged using a corona discharge process in which a large potential is applied across the material causing Paschen breakdown of the gas that fills the voids. The charges generated during breakdown are permanently deposited on the faces of the voids and are opposite in polarity compared to the overall polarity of the outer layer of the material.

Unlike conventional piezoelectric materials in which piezoelectricity is derived from the rotation of dipole moments with applied force, which exist due to the crystalline structure of the material, piezoelectricity in piezoelectret materials occurs due to dimensional changes in the "macroscopic" dipoles, or charged voids. When a positive strain is applied in the thickness direction of a piezoelectret, the thickness increase occurs mainly in the air voids. Increases in the gaps between the charged surfaces of the voids increase the overall macroscopic dipole moment and surface charge, thus producing piezoelectric response and a positive d_{33} coefficient. This behavior is illustrated in Figure 2(b). Due to the nature of the transduction method in piezoelectrets, they have an inherently large d_{33} coefficient but an extremely small d_{31} coefficient, unlike PVDF, which has similar (but opposite) d_{33} and d_{31} coefficients (Measurement Specialties, Inc., 1999).

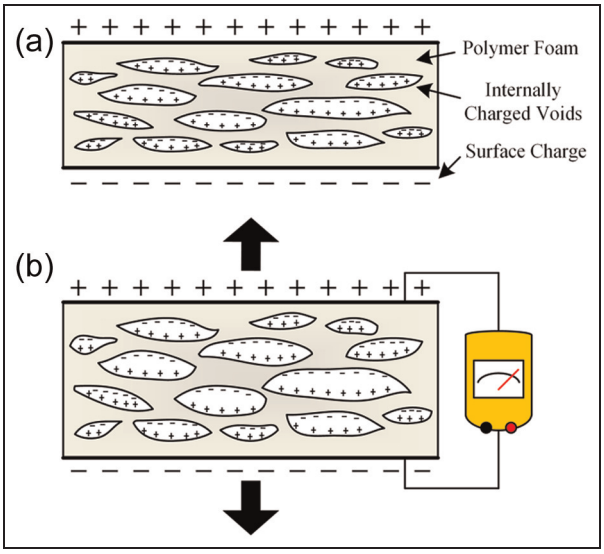

Figure 2. (a) Cross-sectional schematic and (b) piezoelectric behavior of piezoelectret foam.

Mechanical testing

Tensile testing is performed on piezoelectret foam samples both with and without electrodes in order to assess the stiffness and strength of the material in tension. Details are given in the following sections.

Materials

Emfit, Corp. HS-06 (electroded) and HS-06-20BR (non-electroded) piezoelectret films are investigated in this work. The films are manufactured using a continuous biaxial orientation process that stretches the film in two perpendicular directions. Small particulate is introduced to the material before stretching in order to create the lens-like voids in the material after processing. Additionally, a swelling process is performed on the film using a high-pressure gas injection technology. The swelling process increases the material thickness and elasticity in the thickness direction. The thickness of the HS-06 samples is given as 85 μm, while the thickness of the HS-06-20BR samples is given as 97 μm. Corona charging is used to deposit charge into the voids. The manufacturer specifies a piezoelectric constant of $d_{33} = 25 - 250\,\text{pC/N}$, a Young's modulus in the thickness direction of $Y_3 = 0.5\,\text{MPa}$, and an operating temperature from −20°C to +50°C. A photograph of HS-06 films with gold leaf electrodes applied to the surfaces is shown in Figure 3(a).

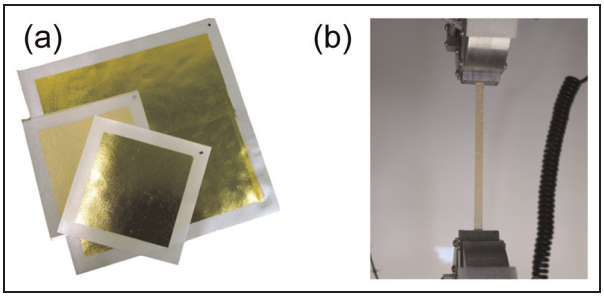

Figure 3. Photographs of (a) HS-06 piezoelectret foam samples and (b) tensile testing experimental setup.

Experimental setup

Tensile testing is carried out using an Instron 1125 Universal Testing frame equipped with a 1 kN load cell and wedge-style grips to hold the samples, as shown in Figure 3(b). The ASTM D 882-10 (2010) (Standard Test Method for Tensile Properties of Thin Plastic Sheeting) was consulted for sample preparation and appropriate test parameters. The standard specifies that uniform samples with a width between 5.0 and 25.4 mm, length between 100 and 250 mm, and width-to-thickness aspect ratio of ≥ 8 should be tested. Additionally, for determination of elastic modulus, the standard specifies that a strain rate of 0.1 mm/mm*min should be used. Given the size of the available samples, specimens of both HS-06 (electroded) and HS-06-20BR (non-electroded) with a width of 9.5 mm and gage length of 76.2 mm were cut from sheets of piezoelectret film using a razor blade. Great care was taken to ensure that smooth, uniform cuts were achieved to prevent any nicks in the edges that could cause premature failure. Eight samples of each material type (four cut in the 1-direction and four cuts perpendicular to the 1-direction, that is, the 2-direction) are tested. Given the sample size and strain rate specification, a crosshead feed rate of 7.62 mm/min was used. Both crosshead displacement and load are recorded throughout each test at a sampling rate of 10 Hz.

Results and discussion

Stress–strain curves recorded during the tensile tests for each specimen are shown in Figure 4. Figure 4(a) presents results from the non-electroded samples, while Figure 4(b) gives results for the electroded samples. From the results, it is clear that the material exhibits strong anisotropy in the principal length directions. The stress–strain behavior for samples cut along the 1-direction is drastically different from the behavior of the samples cut along the 2-direction. This result is likely due to inconsistencies in the biaxial stretching process during manufacturing. If the film is stretched more in a certain direction, then anisotropic behavior should be expected. It should be noted that significant strains, on the order of 35%–150%, are experienced by the materials prior to failure.

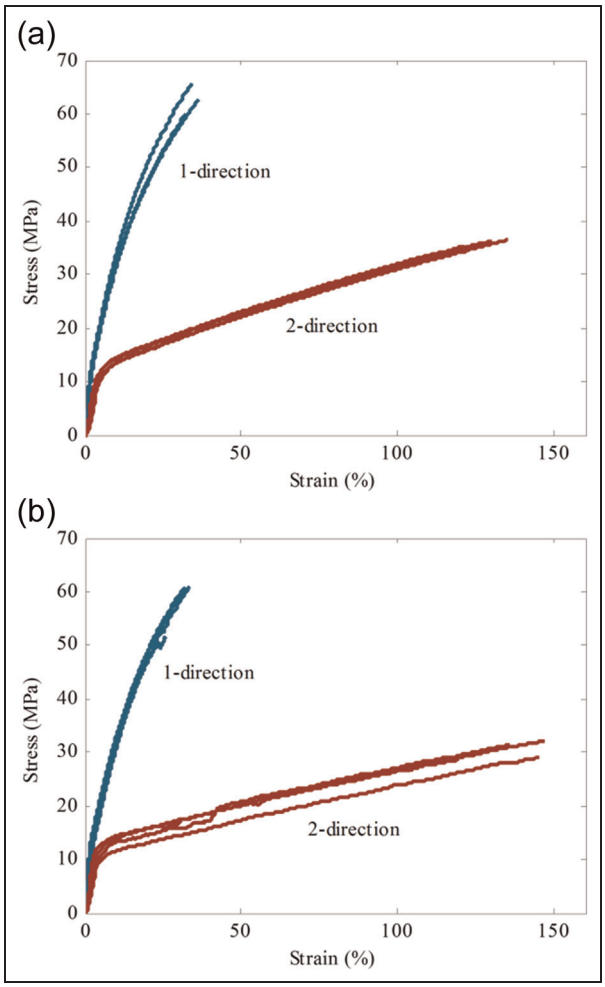

Figure 4. Stress–strain curves for tensile testing of (a) non-electroded and (b) electroded piezoelectret samples.

The average Young's modulus and tensile strength values for all samples tested are given in Table 2. Again, the significant difference between the 1- and 2-directions is apparent from the data. The 1-direction samples exhibit nearly twice the Young's modulus and tensile strength of their 2-direction counterparts. Note that from the limited number of samples tested, it appears as though the addition of gold leaf electrodes does not have a significant effect on the tensile properties and elastic moduli of the foam.

Finally, it can be observed that Young's modulus in the length direction is three orders of magnitude greater than that specified by the manufacturer in the thickness direction ($Y_3 = 0.5$ MPa). This behavior can be easily explained based on the orientation of the voids in the foamed structure (Wegener and Bauer, 2005). Due to the voids, the material is extremely compliant in the

Table 2. Tensile testing results for both electroded and non-electroded samples.

Property	Non-electroded samples		Electroded samples	
	1-direction	2-direction	1-direction	2-direction
Young's modulus (MPa)	990	515	915	560
Tensile strength (MPa)	63	36	60	31

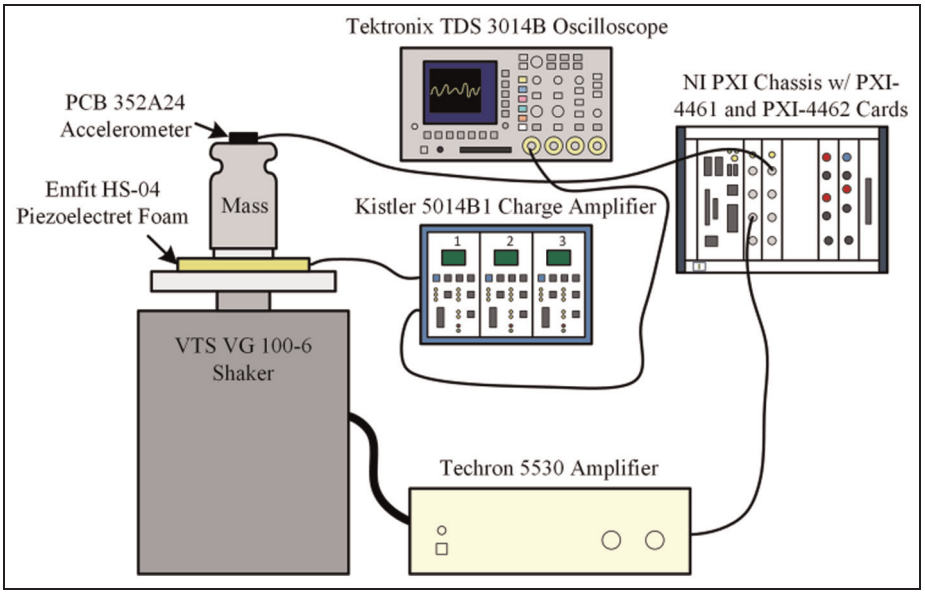

Figure 5. Schematic of experimental test setup used for dynamic d_{33} testing.

thickness direction, which helps allow such large d_{33} values, while much stiffer in the length direction.

Electromechanical testing

Electromechanical testing is performed on the HS-06 (electroded) material in order to measure the dynamic piezoelectric constant, d_{33}, of the foam as a function of frequency. A frequency band up to 1 kHz is chosen for testing to encompass most of the ambient excitation frequencies found in macro-scale energy harvesting systems.

Experimental setup

An experimental setup similar to that used in work published by Hillenbrand and Sessler (2004) and Kressmann (2001) is used in this study. A schematic of the setup can be seen in Figure 5, where an electromagnetic shaker is used to excite a piezoelectret foam sample while monitoring the charge output of the sample. The piezoelectret foam sample tested has dimensions of 5.08 cm × 5.08 cm. An electromagnetic shaker (VG 100-6; Vibration Test Systems, Inc.), and power amplifier (5530, AE Techron, Inc.), is used to drive the sample. The sample is placed on top of a precision ground plate, which is fixed to the shaker armature. A test mass rests on top of a second precision ground adapter plate with dimensions of 2.54 cm × 2.54 cm, which is used to apply pressure to the sample. An accelerometer (PCB 352A24; Piezotronics, Inc.) is placed on top of the mass to measure its acceleration. The output of the accelerometer is measured using an analog input card (PXI-4462; National Instruments Corp.) inserted into a data acquisition system (PXI-1042 chassis and PXI-8186 controller; National Instruments Corp.). Additionally, the excitation signal used to drive the shaker is generated using an analog output card (PXI-4461; National Instruments Corp.) and fed to the power amplifier. The charge generated by the piezoelectret sample is measured directly using a charge amplifier (Type 5010 charge amplifier inserted into 5814B1 chassis; Kistler Group). The output of the charge amplifier is monitored using an oscilloscope (TDS 3014B; Tektronix, Inc.).

When the piezoelectret sample is under excitation, two forces (and corresponding pressures) act on the sample, namely the static force from gravitational acceleration, f_s, and the dynamic force, f_d, associated with the acceleration of the vibrating mass, given as

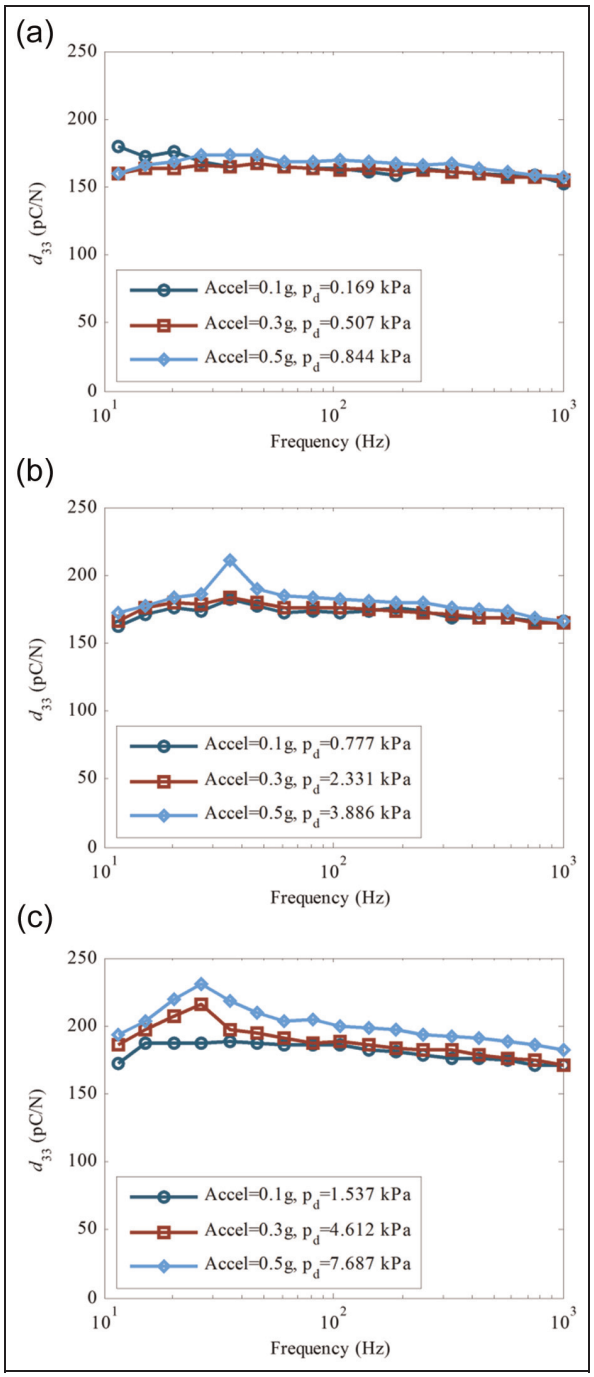

Figure 6. Dynamic d_{33} measurements of piezoelectret foam with (a) 100 g (p_s = 1.69 kPa), (b) 500 g (p_s = 7.77 kPa), and (c) 1 kg (p_s = 15.37 kPa) masses applied.

$$f_s = mg \Rightarrow p_s = \frac{mg}{A}$$
$$f_d = ma \Rightarrow p_d = \frac{ma}{A} \quad (1)$$

where m is the mass, g is the gravitational acceleration, a is the acceleration of the mass, p_s is the static pressure from gravity, p_d is the dynamic pressure from the acceleration of the mass, and A is the area of the adapter plate resting on top of the sample. It should be noted that using this setup, the acceleration of the mass must remain less than the acceleration of gravity to prevent the mass from losing contact with the adapter plate. In this work, the acceleration level is always kept below half of the gravitational acceleration. Large copper tape electrodes with non-conducting adhesive are placed on the surfaces of the precision ground plates to make electrical contact with the sample and to isolate it from the fixture. A frequency range from 10 Hz to 1 kHz is tested. For each point in a particular sweep, the acceleration (dynamic force) is held constant by tuning the output signal to the shaker accordingly. Three different masses (static forces) are tested including 100 g, 500 g, and 1 kg masses. For each mass, three discrete acceleration levels are tested including ± 0.1, ± 0.3, and $\pm 0.5\,g$ peak acceleration.

Results and discussion

Results of the dynamic d_{33} testing are shown in Figure 6. From the results, it can be observed that the d_{33} value remains fairly constant at around 175 pC/N throughout the entire frequency range tested and for all three masses applied. This value falls within the manufacturer specifications of 25–250 pC/N. It should be noted that the peaks observed at around 30–40 Hz in Figure 6(b) and (c) are due to a slight resonance of the fixture and do not represent a resonance of the material. Additionally, the slight increase in d_{33} observed in Figure 6(a) for the $\pm 0.1\,g$ case at low frequencies can be attributed to experimental error when measuring at low frequencies with the given setup. The results of the dynamic d_{33} testing match well with those presented in the literature (Hillenbrand and Sessler, 2004) in which nearly constant values of d_{33} have been reported in this frequency range for similar piezoelectret foam materials.

Energy harvesting investigation

In order to study the energy harvesting capability of piezoelectret foam, both electromechanical modeling and experimental testing are performed. An electromechanically coupled model is first developed to predict the output of a foam sample when excited under biaxial loading. Experimental FRFs are measured and compared to the analytical predictions in order to verify the model. Finally, energy harvesting tests are conducted in which a piezoelectret foam sample is excited harmonically and used to charge a capacitor. Previous work presented by the authors has shown that using the setup given in Figure 5, harmonic excitation of a 5.08 cm × 5.08 cm sample with a 2.54 cm × 2.54 cm

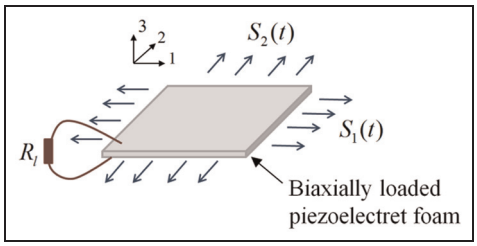

Figure 7. Schematic of piezoelectret energy harvester foam under dynamic biaxial loading.

adapter plate at $\pm 0.5\,g$ acceleration leads to output voltages on the order of 0.1 V across load resistances around 300 kΩ (Anton and Farinholt, 2012). This low output voltage presents a challenge in the development of an energy harvesting system; therefore, excitation of larger samples is investigated in this work with the goal of increasing the output voltage to a usable level.

Electromechanical modeling

Figure 7 shows the schematic of a rectangular piezoelectret energy harvester subjected to dynamic biaxial loading for electrical power generation. The terminals of the conductive electrodes covering the top and bottom surfaces of the foam are connected to a resistive electrical load R_l. At the edges perpendicular to the 1- and 2-directions, the small dynamic strain components $S_1(t)$ and $S_2(t)$ are applied as the source of mechanical excitation. These boundary strain components $S_1(t)$ and $S_2(t)$ are uniform (spatially homogeneous) along their respective edges. The top and bottom faces of the foam (perpendicular to the 3-direction) are traction free and the foam is sufficiently thin to neglect the transverse shear stress components. Therefore, the nonzero stress components are T_1, T_2, and T_6. Assuming linear-elastic behavior, the strain resultant in the thickness direction is nonzero (i.e. $S_3 \neq 0$) due to the Poisson effect and it is given by

$$S_3 = -\frac{\nu_{13}}{Y_1^E} T_1 - \frac{\nu_{23}}{Y_2^E} T_2 \tag{2}$$

where the short-circuit elastic moduli Y_1^E and Y_2^E are assumed to be different to account for the potential orthotropic behavior (e.g. due to uneven static stretching in the 1- and 2-directions in fabrication) and Poisson's ratio terms are defined as $\nu_{ij} = -S_j/S_i$ and they satisfy $\nu_{ij}/Y_i^E = \nu_{ji}/Y_j^E$ $(i,j = 1,2,3)$. The in-plane stresses T_1 and T_2 in equation (2) are

$$T_1 = \frac{Y_1^E}{1-\nu_{12}\nu_{21}} S_1 + \frac{\nu_{21} Y_1^E}{1-\nu_{12}\nu_{21}} S_2 \tag{3}$$

$$T_2 = \frac{\nu_{12} Y_2^E}{1-\nu_{12}\nu_{21}} S_1 + \frac{Y_2^E}{1-\nu_{12}\nu_{21}} S_2 \tag{4}$$

It should be noted that although T_6 (the in-plane twist) might be nonzero, it does not couple with the foregoing equations. Using equations (3) and (4) in equation (2) gives the transverse (thickness direction) strain in terms of the in-plate strain components as

$$S_3 = -\frac{\nu_{13} + \nu_{23}\nu_{12}}{1-\nu_{12}\nu_{21}} S_1 - \frac{\nu_{13}\nu_{21} + \nu_{23}}{1-\nu_{12}\nu_{21}} S_2 \tag{5}$$

Homogeneous strain field is assumed (respectively in the 1- and 2-directions due to the strain components $S_1(t)$ and $S_2(t)$ imposed at the boundaries) to proceed with the energy harvesting derivation. The electric current resultant flowing to the resistor can be obtained from Erturk and Inman (2011) as

$$\frac{d}{dt}\left(\int_A \mathbf{D}\cdot\mathbf{n}\,dA\right) = \frac{v}{R_l} \tag{6}$$

where the nonzero electric displacement (D_3) is given assuming linear piezoelectricity in the reduced (plane-stress) form as

$$D_3 = d_{33} Y_3^E S_3 + \varepsilon_{33}^S E_3 \tag{7}$$

Here, Y_3^E is the short-circuit elastic modulus in the thickness direction, ε_{33}^S is the permittivity component at constant strain, and E_3 is the electric field (which is assumed to be uniform so that $E_3 = -v/h$, where v is the voltage across the resistor and h is the perpendicular distance between the electrodes).

From equations (5) to (7), the form of the dynamic equation that governs the voltage output across the resistor can be obtained as

$$C_p \frac{dv}{dt} + \frac{v}{R_l} = \vartheta_1 \frac{dS_1}{dt} + \vartheta_2 \frac{dS_2}{dt} \tag{8}$$

where C_p is the capacitance of the piezoelectret foam, while ϑ_1 and ϑ_2 are electromechanical coupling constants that depend on the electrode area A, Poisson's ratio terms in equation (5), the elastic modulus Y_3^E, and the piezoelectric constant d_{33}, due to the combination of equations (5) to (7). It is worth mentioning that the first-order representation of the system dynamics given by equation (8) assumes that no resonance takes place in the frequency range of interest and the effect of electrical load on the strain field is negligible.

For harmonic excitation, $S_1(t) = \bar{S}_1 e^{j\omega t}$ and $S_2(t) = \bar{S}_2 e^{j\omega t}$, the voltage output at steady state can be obtained as

$$v(t) = \frac{j\omega(\vartheta_1 \bar{S}_1 + \vartheta_2 \bar{S}_2) e^{j\omega t}}{\frac{1}{R_l} + j\omega C_p} \tag{9}$$

from which the voltage output per strain input FRFs can be extracted as

$$\alpha_1(\omega) = \frac{v(t)}{\bar{S}_1 e^{j\omega t}} = \frac{j\omega\vartheta_1}{\frac{1}{R_l} + j\omega C_p}, \quad \alpha_2(\omega) = \frac{v(t)}{\bar{S}_2 e^{j\omega t}} = \frac{j\omega\vartheta_2}{\frac{1}{R_l} + j\omega C_p} \tag{10}$$

If the nominal lengths of the foam in the 1- and 2-directions are L_1 and L_2, respectively, along with the corresponding small boundary displacements $\delta_1(t) = \bar{\delta}_1 e^{j\omega t}$ and $\delta_2(t) = \bar{\delta}_2 e^{j\omega t}$, the instantaneous homogeneous linear strain components are then $\bar{S}_1 = \bar{\delta}_1/L_1$ and $\bar{S}_2 = \bar{\delta}_2/L_2$. The alternative form of the electromechanical FRFs can therefore be given in the voltage output per displacement input form as

$$\beta_1(\omega) = \frac{v(t)}{\bar{\delta}_1 e^{j\omega t}} = \frac{j\omega\vartheta_1}{\left(\frac{1}{R_l} + j\omega C_p\right)L_1}, \quad \beta_2(\omega) = \frac{v(t)}{\bar{\delta}_2 e^{j\omega t}} = \frac{j\omega\vartheta_2}{\left(\frac{1}{R_l} + j\omega C_p\right)L_2} \tag{11}$$

In the experiments, the boundary displacements $\delta_1(t)$ (in the 1-direction) and $\delta_2(t)$ (in the 2-direction) are measured and the form of the electromechanical FRFs given by equation (11) is employed. The peak power FRF for a given resistance can be obtained from v^2/R_l while the average power is half of the peak power. It should also be clear from equation (11) that the optimal electrical load is $1/\omega C_p$ since first-order behavior (i.e. no resonance) is assumed for the system dynamics in the frequency range of interest.

Experimental setup

The experimental setup used for energy harvesting places a 15.24 cm × 15.24 cm sample of Emfit HS-06 piezoelectret foam in pre-tension and utilizes an electromagnetic shaker to harmonically excite the sample in the length direction about the pre-tensioned state. A schematic and photograph of the setup are shown in Figure 8. Applying pre-tension to the sample ensures that thickness changes will occur in the material for the full stroke of the shaker, thus generating alternating current (AC) voltage when excited sinusoidally. With the fixture design, the sample is first clamped along opposite edges and then loaded into the fixture. Polycarbonate clamps with conductive copper tape strips are used to both clamp and make electrical contact with the sample. With one clamp fixed and the other attached to a linear slide, compression springs placed along guide rods are used to apply pre-tension to the sample. The shaker is then attached to a mounting plate on the linear slide, isolating the shaker armature from the pre-tension load.

Harmonic excitation of the sample is performed using a Labworks ET-126-1 electromechanical shaker powered by a Labworks PA-138 power amplifier. Data acquisition and signal generation are performed using the same NI-PXI system used previously for d_{33} testing. The displacement of the moving clamp is measured using a Keyence LC-2450 laser displacement sensor connected to a Keyence LC2400A controller.

Model verification

Electromechanical FRF measurements are recorded for the system shown in Figure 8 in order to characterize the dynamic response of the piezoelectret foam samples and to verify the electromechanical model. A Brüel & Kjær Photon Dynamic Signal Analyzer is used to generate a chirp excitation signal, which excites the shaker, and also to measure the displacement and output voltage of the sample. Recalling the anisotropy of the material found during tensile testing, the frequency response of the system is measured for two orthogonal orientations of the sample.

The experimental and analytical voltage-to-displacement FRFs for both the 1- and 2-directions are shown in Figure 9. The electromechanical coupling terms in equations (11) are identified for the lowest electrical load for FRFs of the two directions. It should be noted that these directions correspond to those reported previously during tensile testing. In fact, the samples used in tensile testing were cut from the sample used here. From these frequency response results, it is clear that the model provides reasonably accurate predictions of the behavior of the piezoelectret foam samples. It can be observed that the model overpredicts the voltage response of the samples at low frequencies. This discrepancy can be attributed to the fact that accurate experimental measurements of the foam sample at low frequencies are difficult to obtain given the experimental setup used. Specifically, the realization of homogeneous strain components in the experiments is a nontrivial task and fabrication imperfections may also contribute to the nonhomogeneous behavior. Nevertheless, the overall experimental trends are well described by the first-order model given in section "Electromechanical modeling."

For three different excitation frequencies (60, 80, and 100 Hz), the electrical power output (normalized with respect to displacement squared) versus load resistance diagrams is extracted from Figure 9(b) to compare model predictions and experimental measurements for the AC power output. The resulting analytical curves and experimental data points are shown in Figure 10. In addition to reasonable agreement, these measurements also suggest milliwatt-level power output under millimeter-level displacement at the boundaries of the piezoelectret foam used in the experiments based on linear system assumptions.

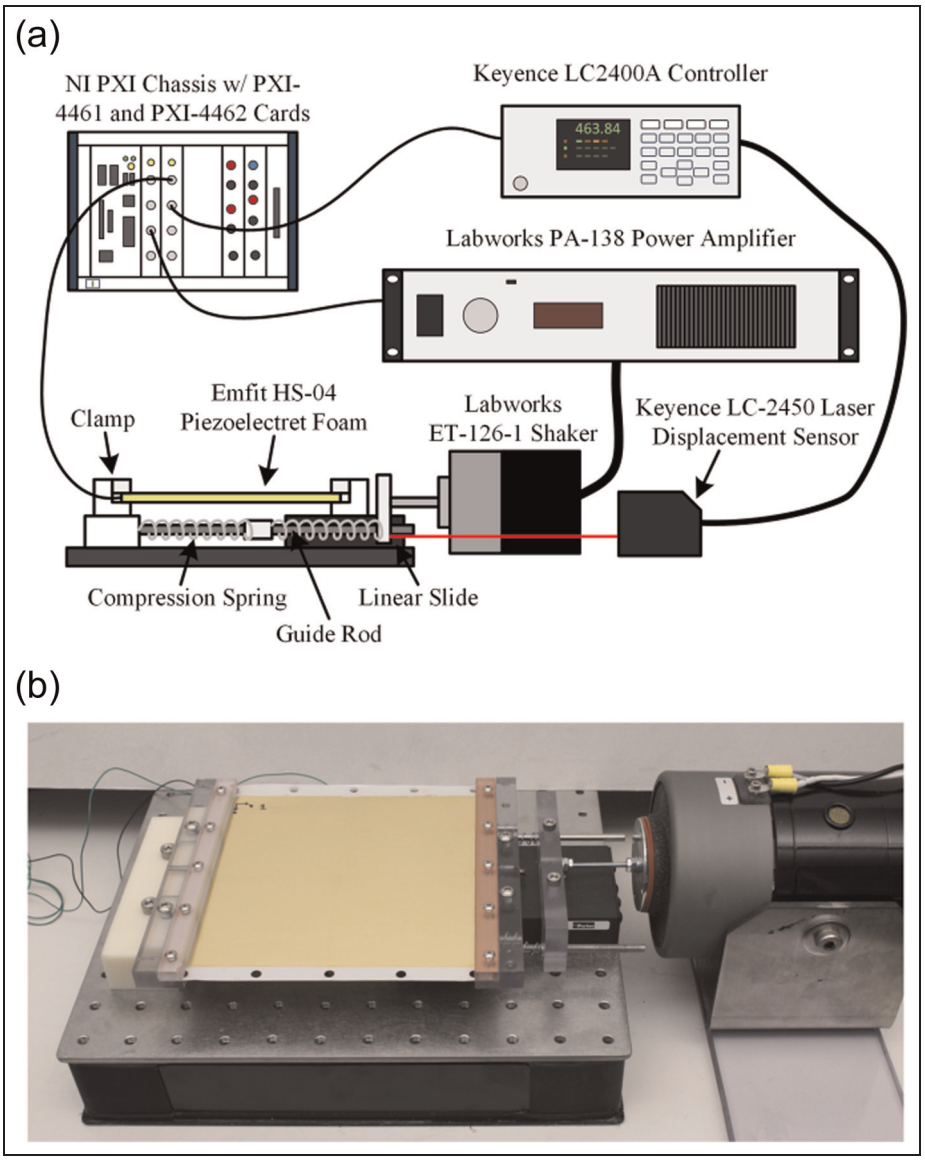

Figure 8. (a) Schematic and (b) photograph of experimental setup used for energy harvesting evaluation.

Capacitor charging experiments

In order to experimentally demonstrate the harvesting abilities of piezoelectret foam, storage experiments (accounting for alternating current-to-direct current (AC-DC) conversion) are conducted in which the output of the sample is connected to a simple full-wave rectifier diode bridge circuit containing a smoothing capacitor and a storage capacitor. Schottky diodes are used to help reduce the forward voltage drop across the bridge. A 0.1 μF electrolytic capacitor serves as a smoothing capacitor and a 1 mF electrolytic capacitor is used for energy storage. Tests are conducted in which the sample is excited along both the 1- and 2-directions in order to compare their performance. In each case, the amplitude of the excitation is tuned to give a fixed displacement of approximately ±73 μm, corresponding to an open-circuit AC voltage of approximately ±8 V in the 1-direction and ±6.75 V in the 2-direction. The excitation frequency is chosen as 60 Hz, and the harvester is allowed to charge the storage capacitor for 30 min. The storage capacitor charge profiles, recorded at 50 Hz sampling rate, are shown in Figure 11. Figure 11(a) compares the measured voltage histories recorded during charging, Figure 11(b) shows the calculated current profiles, and Figure 11(c) shows the calculated power delivered to the capacitors. The results for both orientations match the typical charging profile of a capacitor where the voltage increase is initially rapid and slows as the capacitor becomes charged. Correspondingly, the current peaks initially and tapers off as the test progresses. From the results, it can be seen that excitation in the 1-direction results in more rapid charging of the storage capacitor. A voltage of 4.67 V is

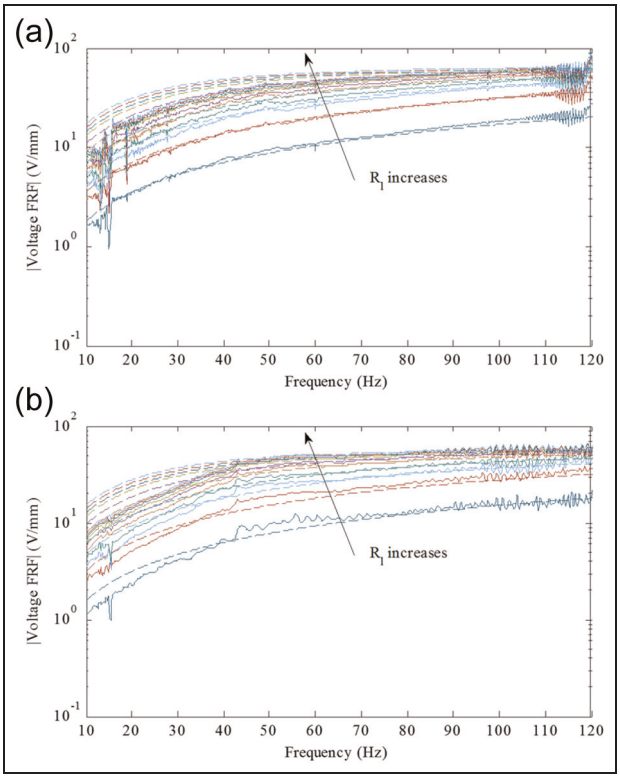

Figure 9. Experimental (solid lines) and analytical (dashed lines) voltage output-to-displacement input frequency response functions for excitation in the (a) 1-direction and (b) 2-direction (for a range of resistance values).

reached after 30 min in the 1-direction, where a voltage of 3.27 is reached in the 2-direction. The average power delivered to the capacitor is calculated as 6.0 and 2.9 μW for the 1- and 2-directions, respectively.

Discussion

Based on the results presented in this section, it is clear that through excitation of a larger sample (on the order of 15 cm × 15 cm), piezoelectret foam is capable of generating enough energy to charge a small capacitor that can be used to power an electronic component. Frequency response measurements show that the material performs differently when excited in orthogonal orientations. In this work, the 1-direction is found superior for energy harvesting purposes.

When excited in the 1-direction at 60 Hz with a displacement of ±73 μm, the piezoelectret foam harvester is able to charge a 1 mF storage capacitor to 4.67 V in just 30 min. This voltage level is adequate for providing power to a variety of electronic devices including wireless sensors. Furthermore, the average power delivered to the capacitor of 6.0 μW is comparable to many conventional piezoceramic and piezoelectric polymer harvester systems (Anton and Sodano, 2007) and is sufficient to provide power to autonomous electronics operating on a duty cycle.

Summary and conclusion

In this work, the use of piezoelectret foam as a novel material for low-level vibration energy harvesting applications is investigated. Piezoelectret foams operate based on changes in their thickness, which cause changes to the macroscopic diploes created during the fabrication process, thereby providing piezoelectric-like response. While a broad range of research has been performed on the characterization and modeling of the material, few studies have investigated the direct use of the large d_{33} coefficient of piezoelectret foams for energy harvesting purposes. In this study, several aspects of the material have been investigated. Tensile testing is performed in order to study the mechanical properties of the foam. Results show that the material is anisotropic in the principal length directions, which is expected to be due to the biaxial loading during fabrication. Young's modulus values between 0.5 and 1 GPa are measured, and tensile strengths between 30 and

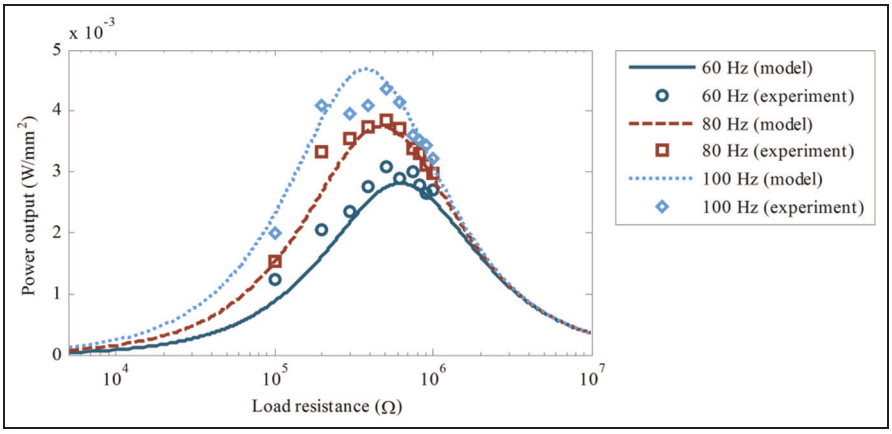

Figure 10. Experimental (markers) and analytical (lines) power output versus load resistance diagrams (normalized with respect to displacement squared) for harmonic excitation in the 2-direction at 60, 80, and 100 Hz.

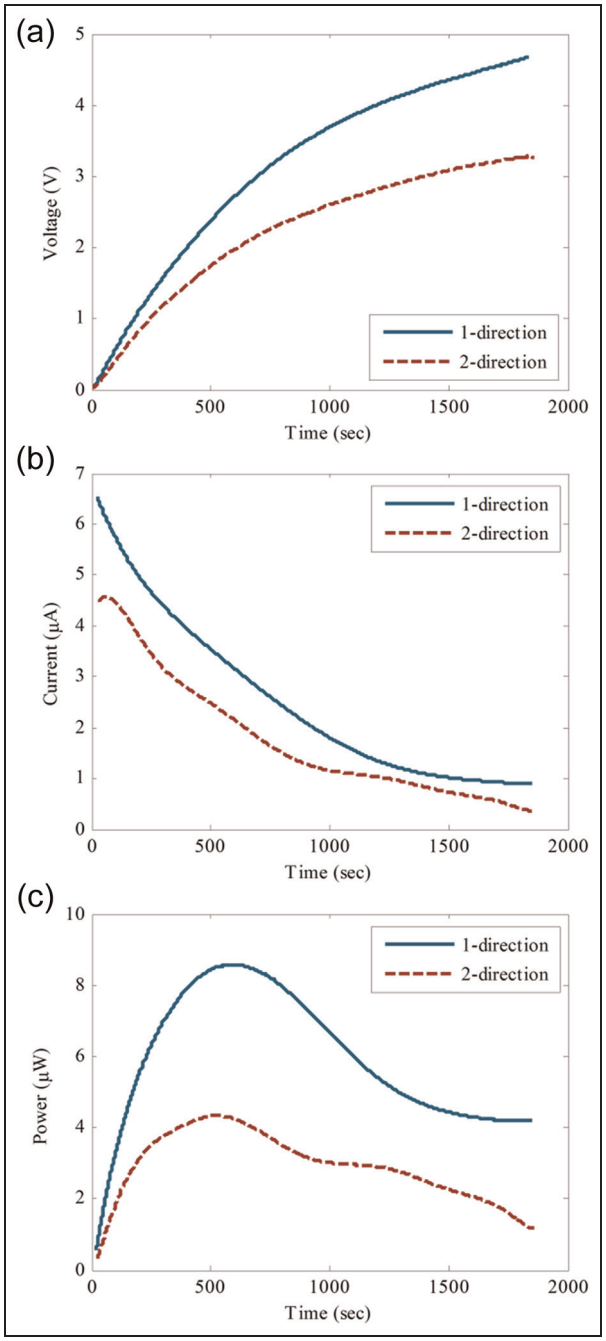

Figure 11. Charging profiles of storage capacitor for excitation at 60 Hz with ±73 μm displacement in the 1- and 2-directions, including (a) measured voltage, (b) calculated current, and (c) calculated power.

65 MPa are found. Electromechanical testing is also performed in order to measure the dynamic d_{33} coefficient of the material under several loading conditions. A relatively constant value of around $d_{33} = 175\,\text{pC/N}$ is found for all combinations of static and dynamic loading over a frequency range from 10 Hz to 1 kHz. The measured trends in d_{33} versus frequency match well with those presented in the literature. Finally, the energy harvesting ability of piezoelectret foam is investigated experimentally and analytically. Initial testing has shown low voltage outputs for small samples excited in the thickness direction (Anton and Farinholt, 2012). In this work, larger pre-tensioned samples are excited in the length direction. An electromechanical model is developed to describe and predict the voltage response of a piezoelectret sample excited harmonically along the length direction. Analytical predictions are compared to experimental FRF measurements and show good correlation. Additionally, FRFs of a foam sample excited in orthogonal directions show that the material performs differently in both orientations, consistent with the anisotropic behavior found in tensile testing. In the preferred orientation, excitation of a 15.2 cm × 15.2 cm sample at 60 Hz with a displacement of ±73 μm yields an average power of 6.0 μW delivered to a 1 mF storage capacitor. The capacitor is charged to 4.67 V in 30 min. This voltage level is sufficient for powering small electronic devices, and the power output of the piezoelectret foam harvester is adequate for providing power to autonomous sensor nodes operating on a duty cycle. In conclusion, piezoelectret foam shows promise for use in low-level vibration energy harvesting applications as a lead-free and extremely compliant alternative to conventional piezoelectric materials.

Acknowledgements

The authors would like to acknowledge the support of Manny Lovato from the Materials Science and Technology Division at Los Alamos National Laboratory for help in conducting the tensile tests presented in this work.

Declaration of conflicting interests

The authors declared no potential conflicts of interest with respect to the research, authorship, and/or publication of this article.

Funding

This work was primarily performed at Los Alamos National Laboratory and was supported by the U.S. Department of Energy through the Los Alamos National Laboratory's Laboratory Directed Research and Development Program.

References

Anton SR and Farinholt KM (2012) An evaluation on low-level vibration energy harvesting using piezoelectret foam. In: *Proceedings of the 19th SPIE annual international symposium on smart structures and materials & nondestructive evaluation and health monitoring* (ed HA Sodano), San Diego, CA, 11 March, paper no. 83410G (10 pp.). Bellingham, WA: SPIE.

ASTM D 882-10 (2010) *Standard Test Method for Tensile Properties of Thin Plastic Sheeting*. West Conshohocken, PA: ASTM International.

Bauer S, Gerhard-Multhaupt R and Sessler G (2004) Ferroelectrets: soft electroactive foams for transducers. *Physics Today* 57: 37–43.

Beeby SP, Tudor MJ and White NM (2006) Energy harvesting vibration sources for microsystems applications. *Measurement Science & Technology* 17: R175–R195.

Boisseau S, Despesse G and Sylvestre A (2010) Optimization of an electret-based energy harvester. *Smart Materials and Structures* 19: 075015 (10 pp.).

Cook-Chennault KA, Thambi N and Sastry AM (2008) Powering MEMS portable devices—a review of non-regenerative and regenerative power supply systems with special emphasis on piezoelectric energy harvesting systems. *Smart Materials and Structures* 17: 043001 (33 pp.).

Erturk A and Inman DJ (2011) *Piezoelectric Energy Harvesting*. Chichester: Wiley.

Gerhard-Multhaupt R (2002) Less can be more. Holes in polymers lead to a new paradigm of piezoelectric materials for electret transducers. *IEEE Transactions on Dielectrics and Electrical Insulation* 9: 850–859.

Hillenbrand J and Sessler GM (2000) Piezoelectricity in cellular electret films. *IEEE Transactions on Dielectrics and Electrical Insulation* 7: 537–542.

Hillenbrand J and Sessler GM (2004) Quasistatic and dynamic piezoelectric coefficients of polymer foams and polymer film systems. *IEEE Transactions on Dielectrics and Electrical Insulation* 11: 72–79.

Hillenbrand J, Sessler GM and Zhang X (2005) Verification of a model for the piezoelectric d_{33} coefficient of cellular electret films. *Journal of Applied Physics* 98: 064105 (5 pp.).

Kressmann R (2001) Linear and nonlinear piezoelectric response of charged cellular polypropylene. *Journal of Applied Physics* 90: 3489–3496.

Measurement Specialties, Inc. (1999) *Piezo Film Sensors*. Hampton, VA: Measurement Specialties, Inc.

Mellinger A, Wegener M, Wirges W, et al. (2006) Thermal and temporal stability of ferroelectret films made from cellular polypropylene/air composites. *Ferroelectrics* 331: 189–199.

Neugschwandtner GS, Schwodiauer R, Bauer-Gogonea S, et al. (2001) Piezo- and pyroelectricity of a polymer-foam space-charge electret. *Journal of Applied Physics* 89: 4503–4511.

Neugschwandtner GS, Schwodiauer R, Vieytes M, et al. (2000) Large and broadband piezoelectricity in smart polymer-foam space-charge electrets. *Applied Physics Letters* 77: 3827–3829.

Paajanen M, Lekkala J and Kirjavainen K (2000a) Electro-Mechanical Film (EMFi)—a new multipurpose electret material. *Sensors and Actuators A: Physical* 84: 95–102.

Paajanen M, Minkkinen H and Raukola J (2002) Gas diffusion expansion-increased thickness and enhanced electromechanical response of cellular polymer electret films. In: *Proceedings of the 11th international symposium on electrets (ISE 11)*, Melbourne, VIC, Australia, 1–3 October, pp. 191–194. New York: IEEE.

Paajanen M, Valimaki H and Lekkala J (1999) Modelling the sensor and actuator operations of the ElectroMechanical Film EMFi. In: *Proceedings of the 10th international symposium on electrets (ISE 10)*, Athens, 22–24 September, pp. 735–738. New York: IEEE.

Paajanen M, Välimäki H and Lekkala J (2000b) Modelling the electromechanical film (EMFi). *Journal of Electrostatics* 48: 193–204.

Paajanen M, Wegener M and Gerhard-Multhaupt R (2001) Understanding the role of the gas in the voids during corona charging of cellular electret films—a way to enhance their piezoelectricity. *Journal of Physics D: Applied Physics* 34: 2482–2488.

Ramadan KS, Sameoto D and Evoy S (2014) A review of piezoelectric polymers as functional materials for electromechanical transducers. *Smart Materials and Structures* 23: 033001. (26 pp.)

Savolainen A and Kirjavainen K (1989) Electrothermomechanical film. Part I. Design and characteristics. *Journal of Macromolecular Science Part A: Chemistry* 26: 583–591.

Sessler GM and Hillenbrand J (1999) Electromechanical response of cellular electret films. In: *Proceedings of the 10th international symposium on electrets (ISE 10)*, Athens, 22–24 September, pp. 261–264. New York: IEEE.

Sodano HA, Inman DJ and Park G (2004) A review of power harvesting from vibration using piezoelectric materials. *The Shock and Vibration Digest* 36: 197–205.

Wegener M and Bauer S (2005) Microstorms in cellular polymers: a route to soft piezoelectric transducer materials with engineered macroscopic dipoles. *ChemPhysChem* 6: 1014–1025.

Zhang X, Hillenbrand J and Sessler GM (2004a) Improvement of piezoelectric activity of cellular polymers using a double-expansion process. *Journal of Physics D: Applied Physics* 37: 2146–2150.

Zhang X, Hillenbrand J and Sessler GM (2004b) Piezoelectric d_{33} coefficient of cellular polypropylene subjected to expansion by pressure treatment. *Applied Physics Letters* 85: 1226–1228.